arXiv:cond-mat/0512495v1 [cond-mat.supr-con] 20 Dec 2005

Vortex-like excitations in a non-superconducting single-layer compound $Bi_{2+x}Sr_{2-x}CuO_{6+\delta}$ single crystal in high magnetic fields

S. I. Vedeneev[1,2] and D. K. Maude[1]
[1] *Grenoble High Magnetic Field Laboratory, Centre National de la Recherche Scientifique, B.P. 166, F-38042 Grenoble Cedex 9, France*
[2] *P.N. Lebedev Physical Institute, Russian Academy of Sciences, 119991 Moscow, Russia*
(Dated: February 2, 2008)

The in-plane $\rho_{ab}(H,T)$ and the out-of-plane $\rho_c(H,T)$ magneto-transport in magnetic fields up to 28 T has been investigated in high quality non-superconducting (down to 20 mK) La-free $Bi_{2+x}Sr_{2-x}CuO_{6+\delta}$ single crystal. By measuring the angular dependence of the in-plane and out-of-plane magnetoresistivities at temperatures from 1 K down to 30 mK, we present evidence for the presence of vortex-like excitations in a non-superconducting cuprate in the insulating state. Such excitations have previously been observed by the detection of a Nernst signal in superconducting cuprates at $T > T_c$ in magnetic fields.

PACS numbers: 74.72.Hs, 74.60.Ec, 74.25.Ey

I. INTRODUCTION

Originating from the pioneering experiments of Uemura *et al.*,[1] there is now a general consensus concerning the determining factor for the critical temperature (T_c) in high- T_c superconductors. In Ref.[1] it was shown that T_c is proportional to the zero-temperature superconducting carrier density for a wide range of underdoped materials. This correlation is a consequence of the proximity to the Mott transition.[2] In conventional superconductors, the destruction of superconductivity begins with the breakup of electron pairs. However, in cuprates with increasing temperature, thermal excitations will destroy the ability of the superconductor to carry a supercurrent whereas the pairs can continue to exist.[3]

At present, there is growing evidence that the transition out of the superconducting state is caused by the proliferation of vortices, which destroy long-range phase coherence. The detection of a large Nernst signal above T_c has provided evidence for the vortex scenario.[3,4,5,6,7] Recently, Sandu *et al.*[8] have shown that the measured in-plane angular dependence of the magnetoresistance on $Y_{1-x}Pr_xBa_2Cu_3O_{7-\delta}$ single crystals with 35 K $\leq T_c \leq$ 92 K is consistent with a flux-flow type contribution. This is again an indication of the presence of vortex-like excitations above T_c in the pseudogap region.

However, in Ref. [9], it has been suggested that the large Nernst signal observed above T_c is due to superconducting fluctuations in the normal state. Very recently, Alexandrov and Zavaritsky[10] calculated the expected Nernst signal in disordered conductors and showed that a strong Nernst signal is unrelated to vortices or a superconducting pair scenario. They found instead, that the Nernst signal could arise from the interference of itinerant and localized-carrier contributions to the thermomagnetic transport.

Therefore, whether these phenomena are a result of the presence of vortices above the zero-field critical temperature remains an open question. Our magnetoresistance investigation of a non-superconducting single crystal at temperature down to 30 mK should help to distinguish between these different points of view because magnetoresistance is a potentially incisive probe of the hole dynamics. In this paper we present, to our knowledge, the first evidence for vortices in a non-superconducting cuprate from angular magnetoresistance measurements on La-free, high quality $Bi_{2+x}Sr_{2-x}CuO_{6+\delta}$ (Bi2201) single crystals. Transport and magnetotransport in non-superconducting Bi2201 crystals have been investigated long ago (see e.g. Refs. [11,12,13,14]), however, magnetoresistance and the angular dependence of the magnetoresistance at mK temperatures was not studied.

In previous measurements[15] we have investigated the in-plane $\rho_{ab}(H,T)$ and the out-of-plane $\rho_c(H,T)$ magneto-transport in magnetic fields up to 28 T in a series of superconducting Bi2201 single crystals over a wide doping range and over a wide range of temperatures down to 40 mK. The T_c(midpoint) values of the crystals lay in the region 2.3 − 9.6 K. With decreasing carrier concentration per Cu atom (p), going from the overdoped ($p = 0.2$) to the underdoped ($p = 0.12$) regimes, a crossover from a metallic to an insulating behavior of $\rho_{ab}(T)$ was observed in the low temperature normal state, resulting from a disorder induced metal insulator transition. Note that, throughout this paper, by insulating phase we simply mean that the resistivity has the temperature dependence of an insulator ($d\rho/dT < 0$) rather than a metal ($d\rho/dT > 0$). The investigations presented in this paper are an extension of these studies to the non-superconducting region of the $H - T$ phase diagram. We used a 28 T resistive magnet at the Grenoble High Magnetic Field Laboratory, in order to measure the in-plane and out-of-plane magnetoresistance with various field orientations relative to the *ab*-plane of the crystal.

II. EXPERIMENT

The preparation and characterization of Bi2201 single crystals are described in detail elsewhere.[15] Here we

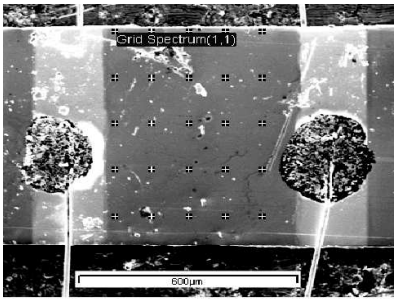

FIG. 1: Scanning electron micrograph of the investigated crystal between voltage contacts where the composition measurement points are denoted by crosses.

have characterized three *as-grown* single crystals which have been grown in the same crucible and found that samples are of high quality with almost identical characteristics. To investigate the low-temperature magnetotransport behavior, we selected the best crystal. The crystal was cut to have the approximate dimensions of 1.9 mm ×0.7 mm×10 μm. The actual cationic composition of the selected sample was measured at 40 different points on the crystal and the scatter in the data was less than 2%. Figure 1 shows the scanning electron micrograph of the crystal between the voltage contacts (gold film, a silver pad and gold wires) where the composition measurement points are denoted by crosses. We estimate the carrier concentration in the sample to be $p = 0.09$ by using the empirical relation between the Bi excess, x, and p.[15,16] Optimum doping in this system occurs around $p \simeq 0.17$ and the $T_c(p)$ dependence shows a faster drop in the underdoped side of the phase diagram. The superconducting phase in B2201 extends only down to $p = 0.11$.[15] The error associated with the carrier concentration estimation is less than 4% (see Fig.1 in Ref. [17]). Thus, our sample with $p = 0.09$ is definitely located below the superconductor-insulator phase transition, heavily underdoped and non-superconducting.[15] The half-width of the sublattice reflections in the X-ray rocking curves for this crystal did not exceed 0.15°. These data clearly demonstrate the high structural quality and high homogeneity of the sample on a microscopic scale.

A four-probe contact configuration, with symmetrical positions of the low-resistance contacts ($< 1\Omega$) on both *ab*-surfaces of the sample was used for the measurements of R_{ab} and R_c resistances. The temperature and magnetic field dependence of the resistances $R_{ab}(T, H)$ and $R_c(T, H)$ were measured using a lock-in amplifier driven at ≈10.7 Hz. For the low temperature magnetotransport measurements, the crystal was placed directly inside the mixing chamber of a top-loading dilution fridge. For the in-plane transport current $\mathbf{J}$, a configuration with $\mathbf{H} \perp \mathbf{J}$ was used in all cases. In the angular magnetoresistance measurements for the out-of-plane transport current, the magnetic field direction changed from the longitudinal ($\mathbf{H} \parallel \mathbf{c} \parallel \mathbf{J}$) to transverse ($\mathbf{H} \perp \mathbf{c} \parallel \mathbf{J}$) configurations. The angular resolution was better than 0.3°. The ac current applied was 5μA for in-plane and 10μA for out-of-plane resistance measurements. A RuO_2 thermometer was used to measure the local temperature of the sample. The field sweep rate $dH/dt = 0.5$ T/min at temperatures 30−150 mK and 1 T/min at higher temperatures was chosen in order to avoid eddy current heating. The temperature was continuously recorded during each measurement sweep.

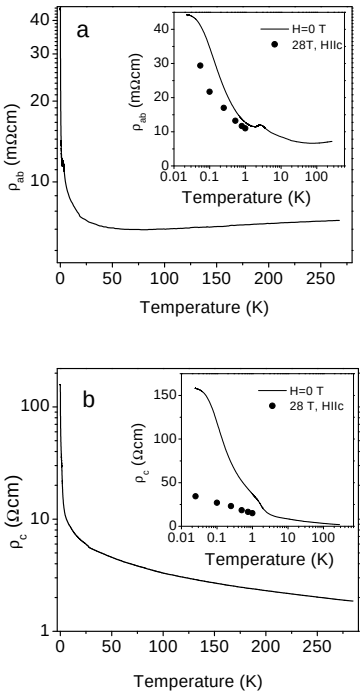

FIG. 2: Temperature dependence of the in-plane ρ_{ab} (a) and out-of-plane ρ_c (b) resistivities for the investigated Bi2201 single crystal. Note the log scale for the vertical axis. The insets plot $\rho_{ab}(T)$ and $\rho_c(T)$ with the horizontal axis plotted using a logarithmic scale in order to emphasize the low-temperature behavior.

III. IN-PLANE $[\rho_{ab}(T)]$ AND OUT-OF-PLANE $[\rho_c(T)]$ RESISTIVITIES

In Fig.2 (main panels) we show the temperature dependence of the in-plane ρ_{ab} (a) and out-of-plane ρ_c (b) resistivities for the investigated Bi2201 single crystal, with the vertical axis plotted using a logarithmic scale. The insets in Fig.2 plot $\rho_{ab}(T)$ and $\rho_c(T)$ with a logarithmic scale for the horizontal axis in order to emphasize the low-temperature behavior. The data points (closed circles) show the resistivity data at $H = 28$ T with the magnetic field parallel to the *c*-axis. Figure 2 clearly demonstrates that at zero magnetic field, the sample remains in its a normal state down to 20 mK. ρ_{ab} in the high-temperature range shows a weak metallic behavior

$(d\rho_{ab}/dT > 0)$, goes through a minimum at temperature $T \approx 70$ K and then shows an insulating behavior, consistent with the onset of localization. $\rho_c(T)$ in Fig.2(b) increases as $\log(1/T)$ as the temperature decreases from the room temperature down to $T \approx 5$ K and then transforms to an insulating behavior. At ultra low temperatures, $T = 0.02 - 0.1$ K, ρ_{ab} and ρ_c show a downward deviation (saturation) from the insulating behavior. Such deviation from a $\log(1/T)$ dependence of the in-plane and out-of-plane resistance of Bi2201 in normal state at ultra low temperatures has been studied in detail in Ref. [15]. As can be seen in Fig.2(a), at zero magnetic field, there is the weak upturn in the region $2 - 3$ K, which in reference [15], was attributed to a competition between the onset of superconductivity and localization. A weak feature in this temperature region is also observed in $\rho_c(T)$ (Fig.2(b)).

A strong 28 T magnetic field in the perpendicular geometry barely suppresses the localization and therefore, the insulating behavior of ρ_{ab} persists [Fig.2(a)] as in the case of underdoped crystals in Ref. [15]. Whereas the effect of the high magnetic field on ρ_c is very noticeable. The insulating behavior of the $\rho_c(T)$ dependence at low temperatures is significantly suppressed and $\rho_c(T)$ shows an almost identical $\log(1/T)$ dependence over the whole temperature range [Fig.2(b)] that can be interpreted as the magnetic-field induced suppression of localization. The behavior of the resistivities described above is in agreement with our previous results for Bi2201 single crystals in the magnetic-field induced normal state[15] and completes the crossover picture from a metallic to an insulating behavior of $\rho_{ab}(T)$ and $\rho_c(T)$ with decreasing hole concentration.

IV. IN-PLANE MAGNETORESISTIVITY $[\rho_{ab}(H)]$

Returning now to the magnetoresistance curves, we immediately encounter an anomaly. Figure 3 (main panel) displays the transverse in-plane magnetoresistance $\rho_{ab}(H)$ for the same Bi2201 sample at various temperatures from 55 mK to 1 K with the magnetic field perpendicular to the *ab*-plane. At each temperature, the magnetic field dependence shows a crossover from positive magnetoresistance at low magnetic field to negative magnetoresistance at higher magnetic fields. As can be seen, the resistivity starts to rise rapidly from the zero-field value, reaches a maximum at the peak field, H_{peak}, and then decreases sharply with increasing magnetic field. Thereafter, the slope $d\rho_{ab}/dH$ changes and becomes small at high field. This behavior points clearly to the presence of two different mechanisms responsible for the negative magnetoresistance in Fig. 3. With increasing temperature, the maximum in $\rho_{ab}(H)$ shifts toward lower magnetic field and the amplitude of the maximum decreases monotonically. It is significant that at low temperature (55 mK) the relative variation $\Delta\rho_{ab}/\rho_{ab0} = [\rho_{ab}(H,T) - \rho_{ab}(0,T)]/\rho_{ab}(0,T)$ is as much

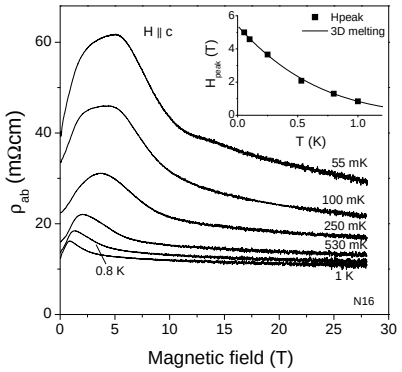

FIG. 3: Transverse in-plane magnetoresistance for Bi2201 sample at various temperatures from 55 mK to 1 K with the magnetic field perpendicular to the *ab*-plane. The inset is the magnetic field position of the maxima $\rho_{ab}(H)$ (squares) versus the temperature. The solid line is a fit to the experimental points using the expression (1) in Ref. [18] for an irreversibility line of our low-T_c Bi2201 single crystals that corresponds to the melting of a three-dimensional vortex lattice (see text below).

as +55% at the peak field (positive magnetoresistance) and -30% at 28 T (negative magnetoresistance) in the transverse configuration of the magnetic field. It should be especially emphasized that the sharp change in the slope $d\rho_{ab}/dH$ in the isotherms occurs at the resistivities near the zero-field values.

For high-T_c superconductors, a small positive transverse and quadratic in-plane magnetoresistance has been observed in $Tl_2Ba_2CuO_{6+\delta}$ (3% at 60 T and 130 K, $T_c \sim 80$ K)[19] and Bi2201 (12% at 8 T and 5 K, $T_c = 3 - 4$ K).[20] However, ρ_{ab} in Fig.3 shows a much stronger positive magnetoresistance compared to reported experimental results and $\Delta\rho_{ab}/\rho_{ab0}$ does not show a quadratic dependence on magnetic field. In quasi-classical models of conventional metals a spin-dependent scattering leads to a very small ($\Delta\rho/\rho \sim 10^{-3}$) positive magnetoresistance. It is known also that the spin-dependent scattering leads to a positive magnetoresistance that is independent of the applied field orientation with respect to the current direction. Thus, *a priori*, the transverse magnetoresistance, in addition to the orbital contribution, may also contain a Zeeman contribution (actually, this is probably not the case, see below).

To understand the origin of the orbital contribution to the transverse in-plane magnetoresistance in our sample, we have studied the angular dependence of the in-plane magnetoresistance. Figure 4 displays the in-plane resistivity as a function of applied field for various magnetic field orientations relative to the *ab*-plane of the crystal, measured at 0.25 (a) and 0.5 K (b). We can clearly see a considerable difference in the field position of the maximum in $\rho_{ab}(H)$ between the perpendicular ($\theta = 90°$) and parallel ($\theta = 0°$) configurations of the magnetic field. Since, in both field directions, the magnetoresistance is transverse, the highly anisotropic response points

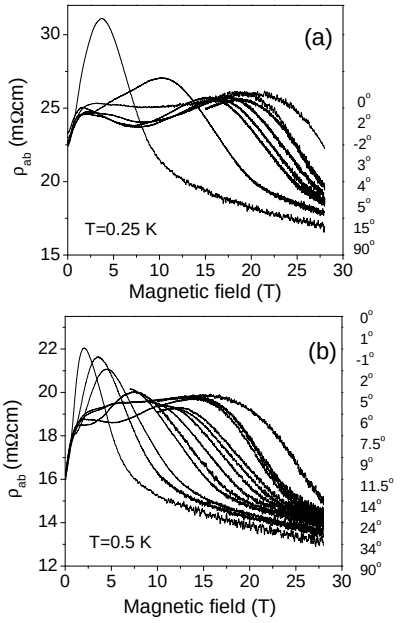

FIG. 4: In-plane resistivity as a function of applied field for various magnetic field orientations relative to the *ab*-plane of the crystal, measured at 0.25 (a) and 0.5 K (b).

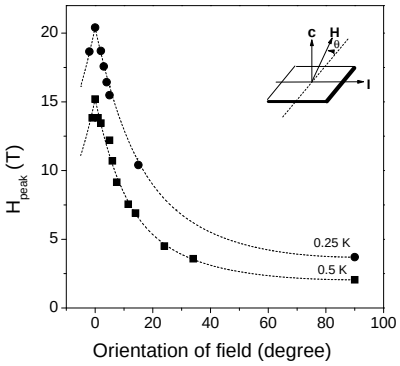

FIG. 5: Angular dependence of the field position of the maximum of $\rho_{ab}(H)$ (H_{peak}) at the temperatures 0.25 and 0.5 K extracted from the magnetoresistance curves in Fig.4. Dashed lines are fits to experimental data using Tinkham's relation with anisotropy parameter $\gamma = H_{c2}^{\parallel ab}/H_{c2}^{\perp ab}$ equals to 5.5 at $T = 0.25$ K and 7.4 at $T = 0.5$ K.

to the importance of orbital effects for the magnetoresistance. This probably excludes any explanation of the positive in-plane magnetoresistance in terms of spin effects. However the large anisotropy is restricted to the region of the peak (the bell-shaped part of the curves) in $\rho_{ab}(H)$. As can be seen from Fig.4, at higher magnetic fields, where $\rho_{ab}(H)$ shows a small negative magnetoresistance, the curves remain almost unchanged as the sample is rotated. Most likely, the high magnetic field region for which $d\rho_{ab}/dH$ is small and negative in Fig.3 and Fig.4, corresponds to the negative transverse in-plane magnetoresistance reported in earlier investigations of non-superconducting Bi2201 single crystals.[14]

The previously reported negative in-plane magnetoresistance was quite small (near 5 % at 0.45 K and 8 T).[14] The magnetoresistance was negative in the temperature range 0.45-20 K and became positive with increasing temperature above 20 K. To account for these results, the authors invoked localization theory,[21] which describes the low-temperature negative magnetoresistance in metals in a weak-localization regime. The negative magnetoresistance resulted from the magnetic field induced suppression of localization effects. In zero magnetic field, samples showed an insulating behavior of $\rho_{ab}(T)$ for $T < 20$ K, where localization effects should be important, especially at very low temperatures. Although the negative in-plane magnetoresistance observed at high magnetic fields in Fig.3 is considerably larger than that observed in Ref. [14] (due to ultra low temperatures), our results are in agreement with these experiments and it is reasonable to assume that they have the same physical origin.

Turning now our attention to the origin of the bell-shaped part of magnetoresistance, we would like to note that in layered superconductors, the anisotropy of the magnetoresistance is a direct consequence of the anisotropy of the upper critical field H_{c2}. In such superconductors with a high degree of anisotropy, a two-dimensional situation with decoupled layers arises and for the angular dependence of H_{c2} it is possible to use Tinkham's relation for a thin-film superconductor in the vicinity of T_c,[22]

$$\mid H_{c2}(\theta)\sin\theta/H_{c2}^{\perp ab} \mid + [H_{c2}(\theta)\cos\theta/H_{c2}^{\parallel ab}]^2 = 1. \qquad (1)$$

In Fig.5, we show the angular dependence of magnetic field position of the maximum of ρ_{ab} at the temperatures 0.25 and 0.5 K extracted from the magnetoresistance of the crystal in Fig.4. Dashed lines are fits to the data using Tinkham's relation, with anisotropy parameter $\gamma = H_{c2}^{\parallel ab}/H_{c2}^{\perp ab}$ equal to 5.5 at $T = 0.25$ K, and 7.4 at $T = 0.5$ K. As can be verified from Fig.5, the magnitudes 5.5 and 7.4 are simply equal to the ratio of the field position of the $\rho_{ab}(H)$ maxima at $\theta = 0°$ and $\theta = 90°$. The experimental points in Fig.5, show a cusp-like behavior at $\theta = 0°$ with $dH_{c2}/d\theta \neq 0$, in good agreement with the prediction of the thin-film model (dashed lines). This cusp-like behavior has previously been observed in superconducting multilayers.[23,24]

Although Tinkham's model predicts a temperature-independent critical-field anisotropy, a temperature dependence is experimentally observed in layered superconducting single crystals .[24,25,26] For comparison, we show in Fig.6 the resistive upper critical field H_{c2}^{*} as a function of the angle between the magnetic field and *ab*-plane at $T = 0.7$ K extracted from the magnetic field-induced transitions of one of our superconducting slightly underdoped Bi2201 single crystals with $T_c = 6-7.5$ K. The different symbols are the experimental H_{c2}^{*} values obtained from the fields at which the resistivity of the sample has reached 1%, 10% and 50% of it normal-state value ρ_n.

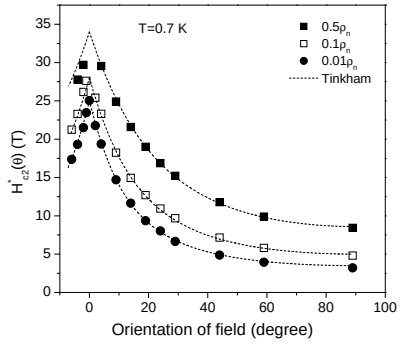

FIG. 6: The resistive upper critical field H^*_{c2} as a function of the angle between the magnetic field and ab-plane at $T = 0.7$ K extracted from the magnetic field-induced transitions of our superconducting slightly underdoped Bi2201 single crystal with $T_c = 6 - 7.5$ K. The different symbols are the experimental H^*_{c2} values obtained from the fields at which the resistivity of the sample has reached 1%, 10% and 50% of it normal-state value ρ_n.

Some data points are missing, because of the very large values of the upper critical fields in the $\mathbf{H}\|\mathbf{ab}$ geometry ($\theta = 0^\circ$) at this temperature, we are unable to determine H^*_{c2} values using the 50% normal-state resistivity criterium. Again, the experimental data, which shows a cusp-like behavior at $\theta = 0$, is in good agreement with the prediction of Tinkham's formula (dashed lines).

In our opinion, Figs.3 - 6 demonstrate clearly that the observed positive in-plane magnetoresistance in ρ_{ab} (Fig.3) is associated with superconductivity and the maximum in $\rho_{ab}(H)$ at low temperatures is close to some "upper critical field". However admittedly, the explanation of the maximum itself in $\rho_{ab}(H)$, in particular the bell-shaped form of the magnetoresistance curves in Fig.3 is not fully understood.

In the inset of Fig.3 we show the magnetic field position of the maxima $\rho_{ab}(H)$ (squares) versus the temperature. The solid line is a fit to the experimental data using expression (1) in Ref. [18] for the irreversibility line of our low-T_c superconducting Bi2201 single crystals which corresponds to the 3D-2D melting of a vortex lattice. Here we have used the fact that at very low temperatures the melting field and the upper critical field coincide[27]. The fit shown in the inset of Fig.3 is made fixing $T_c = 2.45$ K (the onset of the weak upturn in Fig.2(a)) and leaving $H^*_{c2}(0)$ and $c_L^2\sqrt{\beta_m/Gi}$ as free parameters. Here c_L, $\beta_m \approx 5.6$ and Gi are the Lindemann number, a numerical factor and the Ginzburg number, respectively.[18] From the fit we obtain $H^*_{c2}(0) = 5.4$ T and $c_L^2\sqrt{\beta_m/Gi} = 0.37$. The value of $H^*_{c2}(0)$ is close to the experimental magnitude H_{peak}=5 T at $T = 55$ mK and $c_L^2\sqrt{\beta_m/Gi}$ closely matches the value found in Ref. [18] taking into account the difference in "$H^*_{c2}(0)$". This is indicative of the presence of a vortex state in the non-superconducting sample in magnetic field. In this case, the maximum and negative magnetoresistance in the bell-shaped part of $\rho_{ab}(H)$ in Fig.3 can be explained by the fact that at high magnetic fields, the number of regions able to support vortices decreases with increasing magnetic field, and therefore, the dissipation decreases.

A linear extrapolation to high temperatures of the amplitude of the maximum ρ_{ab} plotted on a log scale as a function of temperature (not shown) from Fig.3, shows that the vortex-like excitations have to vanish at a critical temperature $T_\phi \approx 4 - 5$ K. Hence, using $T_c = 2.45$ K for our sample gives $1.5T_c < T_\phi < 2T_c$. This is consistent with the existence of vortex-like excitations in the pseudogap region, up to a temperature T_ϕ, that manifest themselves as flux-flow resistivity.[8]

Another possible explanation for the bell-shaped magnetoresistance in Fig.3, suggested by the quasi-two-dimensional nature of Bi2201, is a magnetic-field-tuned superconductor-insulator transition. Very recently Steiner *et al.*[28] suggested that the behavior of some high-T_c superconductors at very high magnetic fields is similar to that of amorphous indium oxide (InOx) films near the magnetic field tuned superconductor-insulator transition. A similar magnetoresistance peak at low temperatures was first observed by Paalanen *et al.*[29] in amorphous superconducting InOx thin films. The authors of Ref.[29] explained this peak by invoking the scaling theory of the superconductor-insulator transition in disorder two-dimensional superconductors.[30]

In such systems, at sufficiently low magnetic fields and at zero temperature, Cooper pairs are condensed, whereas field-induced vortices can be localized due to disorder (a vortex glass phase). As the magnetic field is increased, the system undergoes a superconductor-insulator transition at some critical field. In the insulating phase, the vortices are delocalized and undergo a condensation, whereas Cooper pairs are localized. Near the transition, there is a competition between condensation of Cooper pairs and vortices. In the vortex-glass phase, long-range crystalline correlations are destroyed by disorder vortex motion at finite temperatures, giving rise to a nonzero resistance. Further increasing the magnetic field causes the system to enter a Fermi-insulator state containing localized single electrons. Experimental evidence for this picture has been provided by the temperature and magnetic-field dependence of the resistance in amorphous InOx films.[29] In order to explain the observed peak in magnetoresistance near the superconductor-insulator transition and the subsequent decrease of the magnetoresistance, it has been suggested that an insulator with localized Cooper pairs should have a higher resistance than an insulator with localized single electrons.

Steiner *et al.*[28] argued that a local pairing amplitude persists well into the dissipative state of the high-T_c superconductors, the regime commonly denoted as the "normal state" in very high magnetic field experiments. They concluded that the superconductor-insulator transition in $La_{2-x}Sr_xCuO_4$ occurs at a critical field of the order of the mean-field upper critical field $H_{c2}(0)$ where the magnetoresistance maximum at low temperatures

was observed.[31] They attributed the magnetoresistance maximum to a decrease in the local pair amplitude and a crossover from a Bose-particle dominated to a Fermi-particle dominated system. This means that the large resistance of the sample is dominated by weakly localized pairs, while above the maximum for $H > H_{c2}(0)$, pairs start to dissociate at a faster rate, giving rise to a negative magnetoresistance as the system slowly approaches a state that does not support pairing.[28]

The magnetoresistance curves presented here in Fig.3 are not strictly identical to those reported for amorphous superconducting InOx films[28,29] in which all isotherms reach a maximum and then start to decrease at a common magnetic field value. In our sample the magnetic field position of the maximum magnetoresistance changes with the temperature. In addition, the resistance of InOx films beyond the maximum saturates at high magnetic field but remains larger by a factor of 1.7 than the zero-field normal-state resistance, as extrapolated from the temperature dependent resistance above the transition. Whereas in our case, the magnetoresistance in the bell-shaped part of the curves reaches the zero-field normal-state value and further decreases at high magnetic field (Fig.3). Nevertheless, the behavior of our strong disordering non-superconducting Bi2201 sample in the low and moderate magnetic fields with the bell-shaped magnetoresistance is similar to that of thin films of amorphous InOx near the magnetic-field-tuned superconductor-insulator transition.[28,29]. Our interest is in the superconductor-insulator transition in a system with a strong disorder which drives $T_c \to 0$ so that bulk superconductivity is suppressed. We note that the description of the superconductor-insulator transition above does not take into account the role of unpaired electrons, which are expected to become important when the magnetic field is high enough to ensure the destruction of the localized pairs. Here, as in Ref. [28], we think that the superconductor-insulator transition in a strongly disordered Bi2201 system occurs close to the mean-field upper critical field $H_{c2}(0)$ where the magnetoresistance in Fig.3 has maximum.

V. OUT-OF-PLANE MAGNETORESISTIVITY $[\rho_c(H)]$

In Fig.7 (main panel) we plot ρ_c versus magnetic field for the same non-superconducting Bi2201 single crystal at various temperatures from 30 mK to 1 K for magnetic field perpendicular to the ab-plane ($\mathbf{H} \parallel \mathbf{c} \parallel \mathbf{J}$). One can see that the longitudinal out-of-plane magnetoresistance is negative over the entire magnetic field region and decreases by almost 80% by $H = 28$ T for $T = 30$ mK. The negative magnetoresistance in Fig.7 rapidly weakens with increasing magnetic field and clearly shows a saturation. These results are surprising because in heavily underdoped superconducting Bi2201 samples, with $p = 0.12$ and 0.13 (T_c(midpoint)=2.3 and 3 K, respectively), after

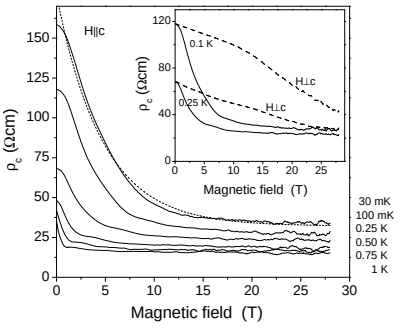

FIG. 7: (Main panel) ρ_c versus magnetic field for Bi2201 single crystal at various temperatures from 30 mK to 1 K for magnetic field perpendicular to the ab-plane ($\mathbf{H} \parallel \mathbf{c} \parallel \mathbf{J}$). The inset is $\rho_c(H)$ curves at temperatures 0.1 and 0.25 K for the longitudinal $\mathbf{H} \parallel \mathbf{c} \parallel \mathbf{J}$ (solid lines) and transverse $\mathbf{H} \perp \mathbf{c} \parallel \mathbf{J}$ (dashed lines) configurations.

the suppression of superconductivity by magnetic field, ρ_c decreases almost linearly with increasing magnetic field by 10-15% at 28 T and 40 mK.[15]

It was found in Ref.[15] that such a behavior of $\rho_c(H)$ is typical for slightly underdoped, optimally doped and overdoped superconducting Bi2201 samples. Moreover, the normal-state out-of-plane magnetoresistance of superconducting samples was independent of the field orientation with respect to the current direction.[32] Whereas, the out-of-plane magnetoresistance in the non-superconducting sample is highly anisotropic. To illustrate this, we show in the inset of Fig.7 the $\rho_c(H)$ curves at temperatures 0.1 and 0.25 K for the longitudinal $\mathbf{H} \parallel \mathbf{c} \parallel \mathbf{J}$ (solid lines) and transverse $\mathbf{H} \perp \mathbf{c} \parallel \mathbf{J}$ (dashed lines) configurations. As in the case of the in-plane magnetoresistance in Fig.4, there is a large difference between the out-of-plane magnetoresistance behavior for two magnetic field orientations relative to the ab-plane of the crystal. This is further evidence that the observed out-of-plane magnetoresistance of the non-superconducting sample may be associated with the superconductivity.

As the response of a superconductor should be to the orbital effect of a magnetic field, we assume following Jing *et al.*,[14] that the longitudinal magnetoresistance involves the spin degrees of freedom alone, and that these contributions are isotropic. Then the orbital contribution to the transverse magnetoresistance may be obtained by subtracting the longitudinal magnetoresistance from the transverse, i.e. $\Delta\rho_{orb} = \Delta\rho_T - \Delta\rho_L$. Here $\Delta\rho_{T,L} = [\rho_c(H,T) - \rho_c(0,T)]/\rho_c(0,T)$. In Fig.8 we display the orbital components of the transverse out-of-plane magnetoresistance at temperatures 0.1 and 0.25 K extracted from the data in the inset of Fig.7. The curves in Fig.8 are remarkably similar to the broad interlayer resistive transitions of the superconducting Bi2201 single crystals in the transverse configuration of the magnetic field ($\mathbf{H} \perp \mathbf{c} \parallel \mathbf{J}$). For comparison, we show in the inset of Fig.8 the field dependence of the out-of-plane resistiv-

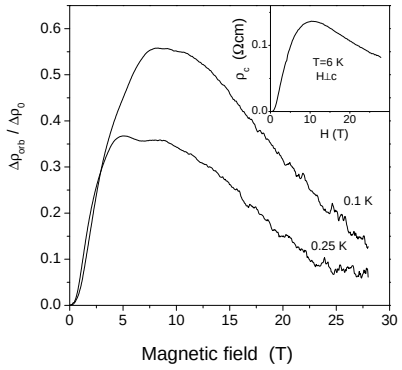

FIG. 8: Orbital components of the transverse out-of-plane magnetoresistance at temperatures 0.1 and 0.25 K extracted from the data in the inset of Fig.7. The inset displays the field dependence of the out-of-plane resistivity ρ_c in the transverse configuration for our optimaly doped Bi2201 single crystal with $T_c = 9.5$ K (midpoint).[32]

ity ρ_c in the transverse configuration for our optimaly doped Bi2201 single crystal with T_c(midpoint)= 9.5 K.[32]

Turning back to Fig.7 (main panel), we see that the out-of-plane negative magnetoresistance at ultra low temperatures rapidly saturates with a characteristic exponential decrease with magnetic field. The short dashed curve shows a numerical fit to the magnetoresistance data at 30 mK calculated using the functional form $\rho_c(H,T) = \rho_{c0} + a\exp(-H/bT)$, where a and b are constants. In previous measurements[15] we have pointed out that this Zeeman-like expression describes the anisotropic negative out-of-plane magnetoresistance in the superconducting Bi2201 samples, where, the major contribution to the $\rho_c(H)$ curves is due to the gradual decrease of the superconducting gap. If we suggest that a vestige of superconductivity exists in the non-superconducting sample, then a comparison of the temperature-dependent data in Fig.2(b) with the data in Fig.7, allows us to conclude that the observed negative magnetoresistance corresponds to a suppression of the insulating behavior in $\rho_c(T)$, which can in turn be interpreted as the magnetic-field induced suppression of the superconducting gap. This is simply a consequence of the fact that Cooper pairs exist at low temperatures in our non superconducting sample, while bulk superconductivity is suppressed by strong disorder.

The data in Fig.5 suggest that the "depairing" field $H_{c2}^{\|ab}$ in the parallel ($\theta = 0°$) configuration of the magnetic field at 0.25 K is 20.5 T. In previous measurements[15,33] we have shown that the maximum in $\rho_c(H)$ for Bi2201 single crystals does not coincide with H_{c2} and that is positioned near $0.4\rho_{ab}^n$, where ρ_{ab}^n is the normal-state resistivity in ab-plane. Moreover, the $\rho_c(H)$ curves have a pronounced break-point in the derivative well above the $\rho_c(H)$ peak. The field position of these break-points in the derivative coincide with the H_{c2} values determined from the $\rho_{ab}(H)$ curves.[33] As can be seen in Fig.8, the orbital components of the transverse out-of-plane magnetoresistance ($\theta = 0°$) at temperature 0.25 K also start to saturate at $H \simeq 22$ T. The fact that "$H_{c2}^{\|ab}$ magnitudes" found from the in-plane and out-of-plane magnetoresistance are in close agreement further supports the presence the vortex-like excitations in the heavily underdoped non-superconducting Bi2201 sample.

Regarding the large negative longitudinal magnetoresistance we note that an anomalously large negative longitudinal magnetoresistance (almost 90 % at 50 mK and 8 T) has been observed previously in the transition metal dichalcogenides[34] which also have a layered structure. These compounds show a typical temperature dependence characteristic of variable-range hopping between localized states. Fukuyama and Yosida[35] have explained this phenomenon by introducing Zeeman shifts for the Anderson localized states leading to enhanced conductivity (exponential in $g\mu_B H/k_B T$) with the energy levels of one spin component closer to the mobility edge. Here the g is the Landé g-factor and μ_B is the Bohr magneton. Since our sample shows an insulating behavior for $\rho_{ab}(T)$ [Fig.2(a)], we cannot exclude that the large negative longitudinal magnetoresistance in Fig.7 has the same origin as in Ref.[34].

Thus, there are strong grounds to believe that the data above indicates a link between superconductivity and the observed magnetoresistance of the non-superconducting sample. We can formally exclude macroscopic sample inhomogeneity, as the origin of the observed phenomena because the crystal is of a very high quality, judging from the magnetization measurements, composition analysis and X-ray measurements. The composition of the crystal was studied using a Philips CM-30 electron microscopy with a Link analytical AN-95S energy dispersion X-ray spectrometer that permitted to study sample across the whole thickness (10 μm). Since the X-ray penetration depth in the X-ray diffraction measurements was nearly 6.5 μm, the crystal was investigated on both sides. The rocking curve width, was also found to be identical.

Taken together, the evidence suggest that at high magnetic field, the sample, in an insulating state, is populated by vortices as observed in superconducting cuprates at $T > T_c$ in a magnetic field, for example, by the detection of a large Nernst signal,[3,4,5,6,7] angular magnetoresistivity measurements,[8] and a torque magnetometry.[36] In a strongly disordered superconductor in zero magnetic field at very low temperatures, localization effects are strong, long-range phase coherence is destroyed and the superconductivity is suppressed. Nevertheless, a vestige of superconductivity and delocalized vortex-like excitations exist in a magnetic field.[3] Vortex motion at finite temperatures leads also to a nonzero positive magnetoresistance (Fig.3 and Fig.4). In the vicinity of the maximum in $\rho_{ab}(H)$ a melting of the vortices occurs resulting in a competition between the positive magnetoresistance and the negative in-plane magnetoresistance that is due to delocalized unpaired electrons. The negative magnetoresistance is also caused by the decrease of the number of regions able to support vortices with increasing

the magnetic field. Since the pair amplitude of localized Cooper pairs is very slowly suppressed out to high magnetic fields, the system retains a vestige of superconductivity at magnetic fields well above H_{c2}.[28] The system slowly approaches a state that does not support pairing where the bell-shaped part of $\rho_{ab}(H)$ curves in Fig.3 is completed. Thereafter the negative in-plane magnetoresistance is due to the magnetic field dependent localization effects only.

VI. CONCLUSION

We have presented the temperature dependence for both the in-plane $\rho_{ab}(T)$ and out-of-plane $\rho_c(T)$ resistivities and magnetoresistivities $\rho_{ab}(H)$ and $\rho_c(H)$ in a high quality non-superconducting (down to 20 mK) La-free $Bi_{2+x}Sr_{2-x}CuO_{6+\delta}$ single crystal. The metallic behavior of $\rho_{ab}(T)$ gradually changes to insulating behavior with decreasing temperature consistent with the onset of localization. $\rho_c(T)$ increases as $\log(1/T)$ as the temperature decreases from room temperature down to $T \approx 5$ K and then transforms to an insulating behavior down to 20 mK also due to localization. A strong 28 T-magnetic field in the perpendicular geometry barely suppresses of the insulating behavior of ρ_{ab}. Whereas magnetic field effectively suppresses the insulating behavior in $\rho_c(T)$ at low temperatures and $\rho_c(T)$ shows an almost identical $\log(1/T)$ dependence over whole temperature range. Again, this can be interpreted as the magnetic-field induced suppression of localization. By measuring the angular dependencies of in-plane and out-of-plane magnetoresistivities at temperatures from 1 K down to 30 mK, we have obtained evidence for the presence of vortex-like excitations in a non-superconducting cuprate in the insulating state. Similar vortex-like excitations have been previously observed in superconducting cuprates at $T > T_c$ in magnetic fields by the detection of a Nernst signal.

Acknowledgments

We thank V.P. Martovitskii and S.G. Chernook for the careful characterization of the single crystals. This work has been partially supported by NATO grant PST.CLG. 979896.

[1] Y. J. Uemura *et al.*, Phys. Rev. Lett. **62**, 2317 (1989).
[2] J. Orenstein and A. J. Millis, Science **288**, 468 (2000).
[3] Z. A. Xu, N. P. Ong, Y. Wang, T. Kakeshita, and S. Uchida, Nature (London) **406**, 486 (2000).
[4] J. Corson, R. Mallozzi, J. Orenstein, J. N. Eckstein, and I. Bozovic, Nature (London) **398**, 221 (1999).
[5] C. Capan, K. Behnia, J. Hinderer, A. G. M. Jansen, W. Lang, C. Marcenat, C. Marin, and J. Flouquet, Phys. Rev. Lett. **88**, 056601 (2002).
[6] Y. Wang, N. P. Ong, Z. A. Xu, T. Kakeshita, S. Uchida, D. A. Bonn, R. Liang, and W. N. Hardy, Phys. Rev. Lett. **88**, 257003 (2002).
[7] Y. Wang, S. Ono, Y. Onose, G. Gu, Y. Ando, Y. Tokura, S. Uchida, and N. P. Ong, Science **299**, 86 (2003).
[8] V. Sandu, E. Cimpoiasu, T. Katuwal, S. Li, M. B. Maple, and C. C. Almasan, Phys. Rev. Lett. **93**, 177005 (2004).
[9] S. Tan and K. Levin, Phys. Rev. B **69**, 064510 (2004).
[10] A. S. Alexandrov and V. N. Zavaritsky, Phys. Rev. Lett. **93**, 217002 (2004).
[11] S. Martin, A. T. Fiory, R. M. Fleming, L. F. Schneemeyer, and J. V. Waszczak, Phys. Rev. B **41**, 846 (1990).
[12] A. T. Fiory, S. Martin, R. M. Fleming, L. F. Schneemeyer, J. V. Waszczak, and R. Reeder, Phys. Rev. B **41**, 2627 (1990).
[13] L. Forro, D. Mandrus, C. Kendziora, L. Mihaly, and R. Reeder, Phys. Rev. B **42**, 8704 (1990).
[14] T. W. Jing, N. P. Ong, T. V. Ramakrishnan, J. M. Tarascon, and K. Remschnig, Phys. Rev. Lett **67**, 761 (1991).
[15] S. I. Vedeneev and D. K. Maude, Phys. Rev. B **70**, 184524 (2004).
[16] Y. Ando, Y. Hanaki, S. Ono, T. Murayama, T. Segawa, N. Miyamoto, and S. Komiya, Phys. Rev. B **61**, R14956 (2000).
[17] R. Bel, K. Behnia, C. Proust, P. van der Linden, D. Maude, and S. I. Vedeneev, Phys. Rev. Lett **92**, 177003 (2004).
[18] A. Morello, A. G. M. Jansen, R. S. Gonnelli, and S. I. Vedeneev, Phys. Rev. B **61**, 9113 (2000).
[19] A. W. Tyler, Y. Ando, F. F. Balakirev, A. Passner, G. S. Boebinger, A. J. Schofield, A. P. Mackenzie, and O. Laborde, Phys. Rev. B **57**, 728 (1998).
[20] S. I. Vedeneev, A. G. M. Jansen, and P. Wyder, Zh.Eksp.Teor.Fiz. **117**, 1198 (2000), [Sov. Phys. JETP, **90**, No 6,1042-1049 (2000)].
[21] P. A. Lee and T. V. Ramakrishnan, Rev. Mod. Phys. **57**, 287 (1985).
[22] M. Tinkham, Phys. Rev. **129**, 2413 (1963).
[23] B. Y. Jin, J. B. Ketterson, E. J. McNiff, S. Foner, and I. K. Schuller, J. Low Temp. Phys. **69**, 39 (1987).
[24] A. K. Ghosh, M. Tokunaga, and T. Tamegai, Phys. Rev. B **68**, 054507 (2003).
[25] S. I. Vedeneev and Y. N. Ovchinnikov, JETP Lett. **75**, 195 (2002).
[26] P. Samuely, P. Szabo, J. Kacmarcik, A. G. M. Jansen, A. Lafond, A. Meerschaut, and A. Briggs, Physica C **369**, 61 (2002).
[27] T. Shibauchi, L. Krusin-Elbaum, G. Blatter, and C. H. Mielke, Phys. Rev. B **67**, 064514 (2003).
[28] M. A. Steiner, G. Boebinger, and A. Kapitulnik, Phys. Rev. Lett. **94**, 107008 (2005).
[29] M. A. Paalanen, A. F. Hebard, and R. R. Ruel, Phys. Rev. Lett. **69**, 1604 (1992).
[30] M. P. A. Fisher, Phys. Rev. Lett. **65**, 923 (1990).
[31] Y. Ando, G. Boebinger, A. Passner, T. Kimura, and K. Kishio, Phys. Rev. Lett. **75**, 4662 (1995).
[32] S. I. Vedeneev, A. G. M. Jansen, and P. Wyder, Phys. Rev. B **62**, 5997 (2000).
[33] S. I. Vedeneev, A. G. M. Jansen, E. Haanappel, and P. Wyder, Phys. Rev. B **60**, 12467 (1999).

[34] N. Kobayashi and Y. Muto, Solid State Commun. **30**, 337 (1979).
[35] H. Fukuyama and K. Yosida, J. Phys. Soc. Jpn. **46**, 102 (1979), *ibid* 1522 (1979).
[36] Y. Wang, L. Li, M. J. Naughton, G. D. Gu, S. Uchida, and N. P. Ong, Cond-mat/0503190 (2005).